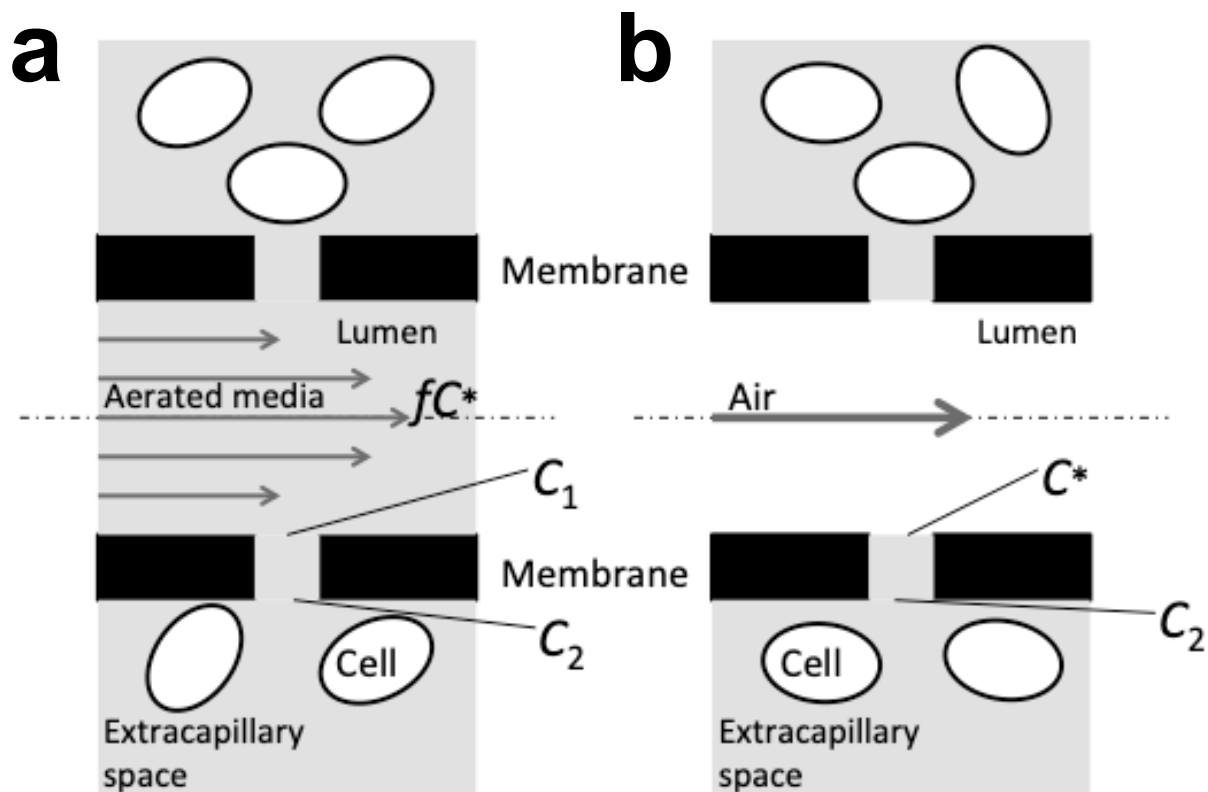


**Supplemental Figure 1. Schematic of T cell culture conditions.** *Panel a* outlines the steps of the T cell manufacturing. *Panel b* highlights the transfer of the T cell culture into ever larger vessels during the upscale process. *Panel c* highlights the "one-pot" solution offered by the HFMBR. The new operating mode is explained using the *blue arrows* to denote the input of fresh medium and the *red arrows* to denote the expulsion of the spent medium via perfusion. The *grey arrow* highlights the gas exchange across the hollow fiber.



**Supplemental Figure 2. Schematic of mass transfer of oxygen in HFMBR.** The schematics above represent the conventional mode of operation (*Panel a*) and our novel operation model (*Panel b*). In both cases, cells (shown as *white ovals*) are located in the extracapillary space. In the case of the conventional model (*Panel a*), medium is aerated outside of the bioreactor and oxygen is delivered to the cells via the aerated medium that passes through the membrane lumen. In the case of our novel operating mode (*Panel b*), incubator air is drawn through the membrane lumen and oxygen passes through membrane into the culture medium. The mechanism of oxygen transfer is the key difference in this operation mode.

The flux of oxygen from the bulk media on the lumen side to the surface of the membrane is:

$$J_{Oxy} = k_L (fC^* - C_1) \quad (1)$$

Where  $0 < f < 1$

The flux of oxygen across the membrane is:

$$J_{OxyM} = \frac{D}{\delta} (C_1 - C_2) \quad (2)$$

The theoretical peak oxygen flux through the membrane corresponds to a condition where all available oxygen is immediately consumed on the intra-capillary space, i.e. a perfect sink condition where  $C_2 \cong 0$ .

Therefore:

$$\left[ J_{OxyM}^{\max} \right]_{Conventional} = \frac{DC_1}{\delta} \quad (3)$$

For direct oxygenation through the membrane, the theoretical peak oxygen flux is given by:

$$\left[ J_{OxyM}^{\max} \right]_{Direct} = \frac{DC^*}{\delta} \quad (4)$$

Now  $C^* > fC^* > C_1$

Therefore:

$$\left[ J_{OxyM}^{\max} \right]_{Direct} > \left[ J_{OxyM}^{\max} \right]_{Conventional} \quad (5)$$

If the flux of oxygen through the membrane is the rate limiting step, from equations (1) and (3):

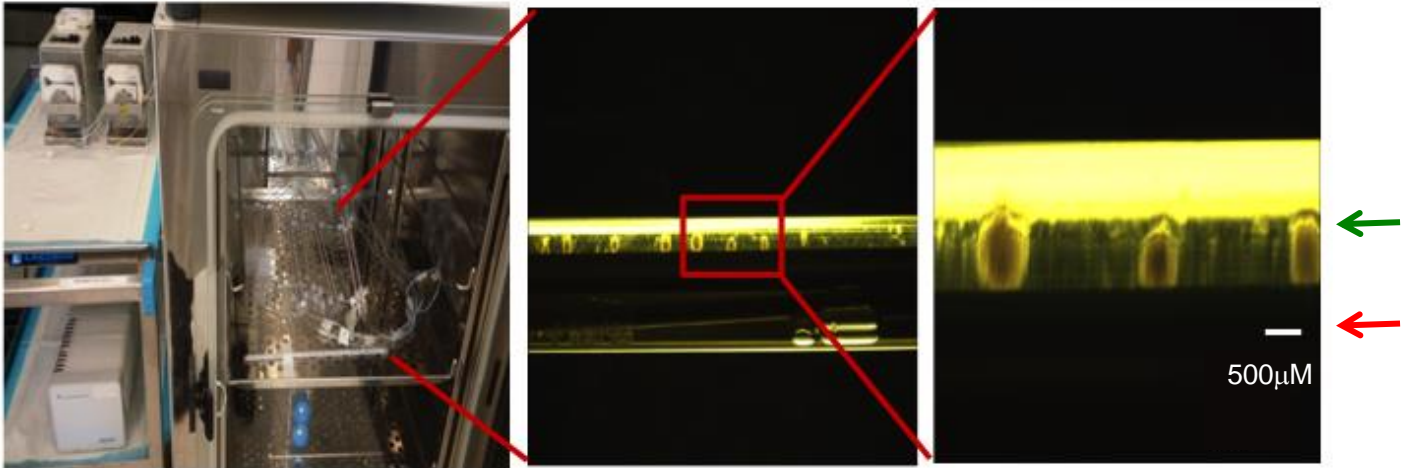
$$C_1 = \frac{k_L \delta f C^*}{D + k_L \delta} \quad (6)$$

From equations (3), (4) and (6):

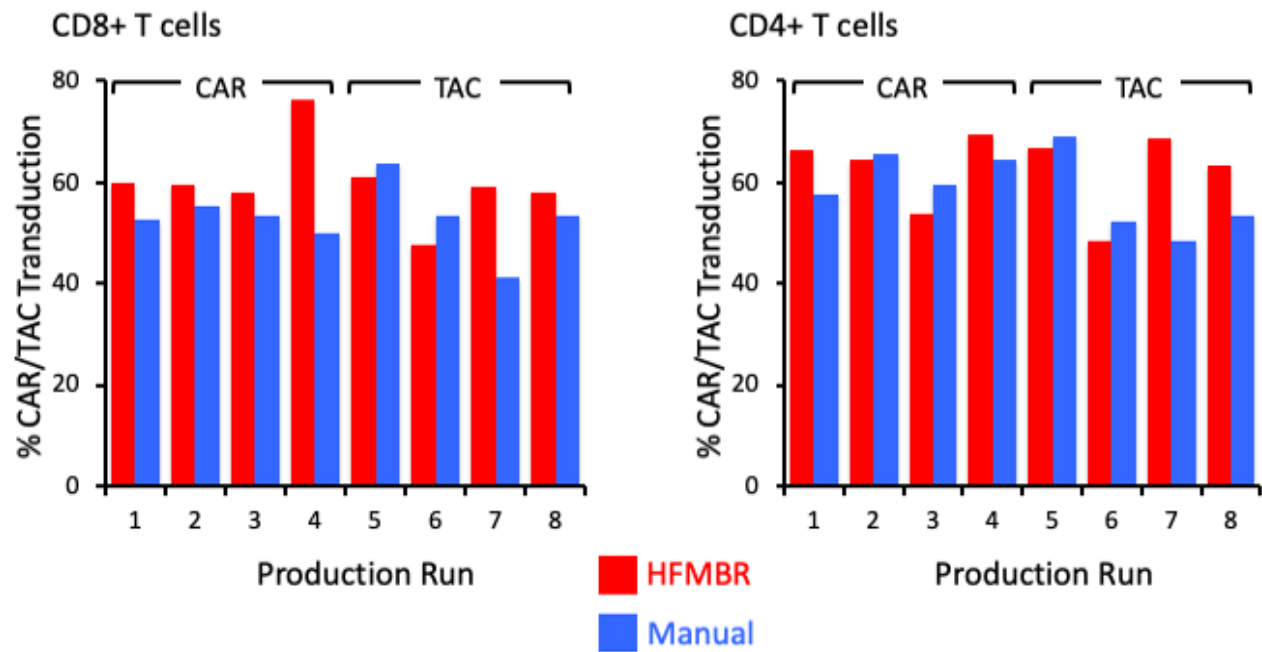
$$\frac{\left[ J_{OxyM}^{\max} \right]_{Direct}}{\left[ J_{OxyM}^{\max} \right]_{Conventional}} = \frac{1 + \frac{D}{k_L \delta}}{f} \quad (7)$$

As the numerator of the RHS is always greater than 1 while the denominator is less than 1,  $\left[ J_{OxyM}^{\max} \right]_{direct}$  will always be greater than  $\left[ J_{OxyM}^{\max} \right]_{Conventional}$ .

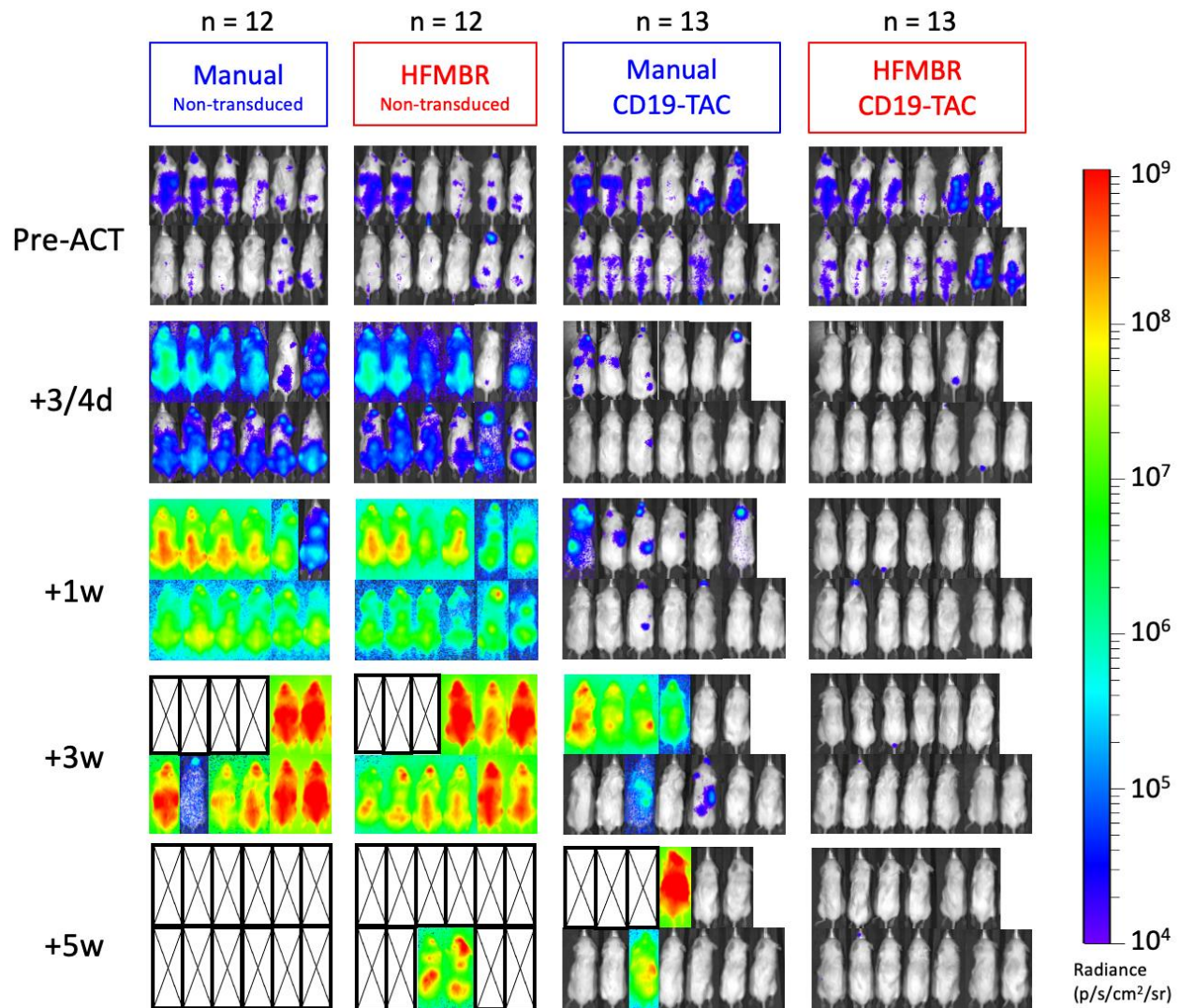
**Supplemental Figure 3. Equations governing oxygen transport in HFMBR.** The equations above relate to terms ( $C_1$ ,  $C_2$ ,  $C^*$ ,  $fC^*$ ) shown in Supplemental Figure 2.



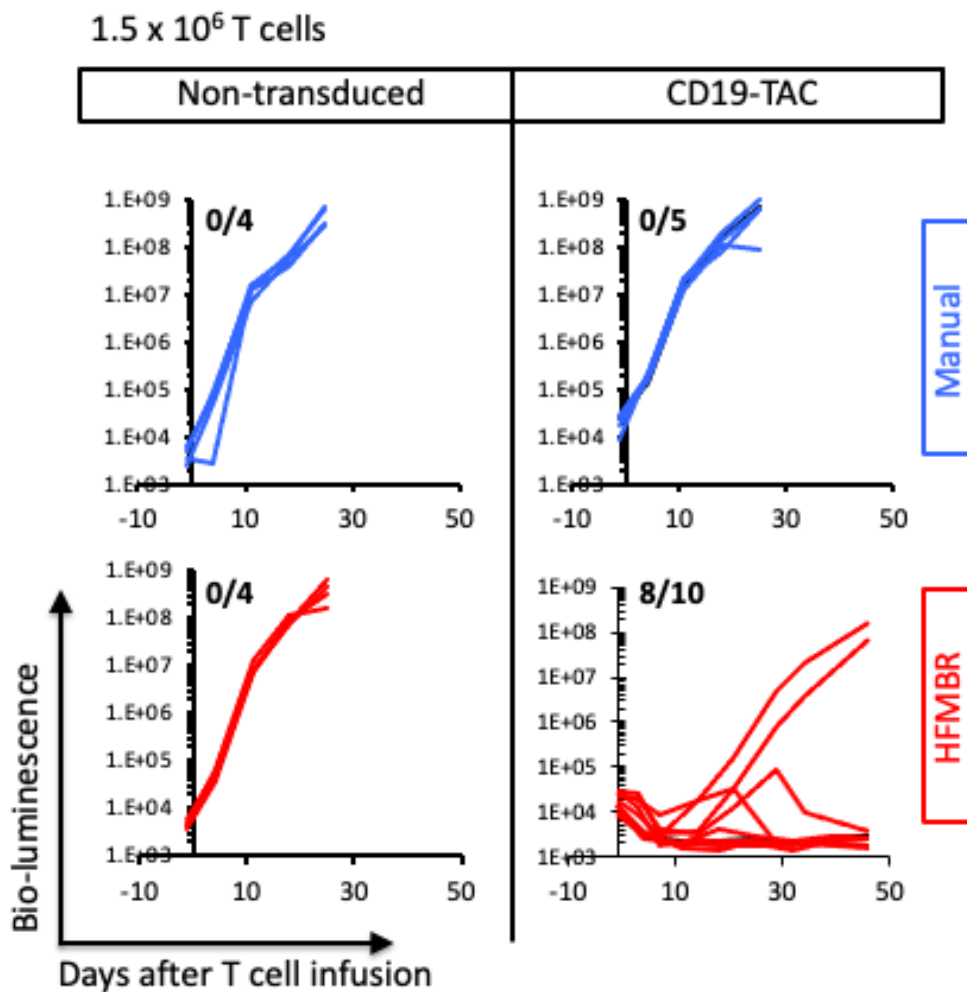
**Supplemental Figure 4. Images of HFMB set up.** *Panel A* Hollow fiber membrane bioreactors were placed in a conventional incubator. The bioreactors were connected to medium and waste reservoirs through C-Flex tubing that were located on the exterior of the incubator. Gas and fluid flow were managed by peristaltic pumps located on the exterior of the incubator. *Panel B* shows T cells growing as clusters within the hollow fiber membrane bioreactor. *Panel C* is an expanded view of the bioreactor shown in *Panel B*. The T cell clusters (*green arrow*) are very close to the hollow fiber (*red arrow*) facilitating gas exchange.



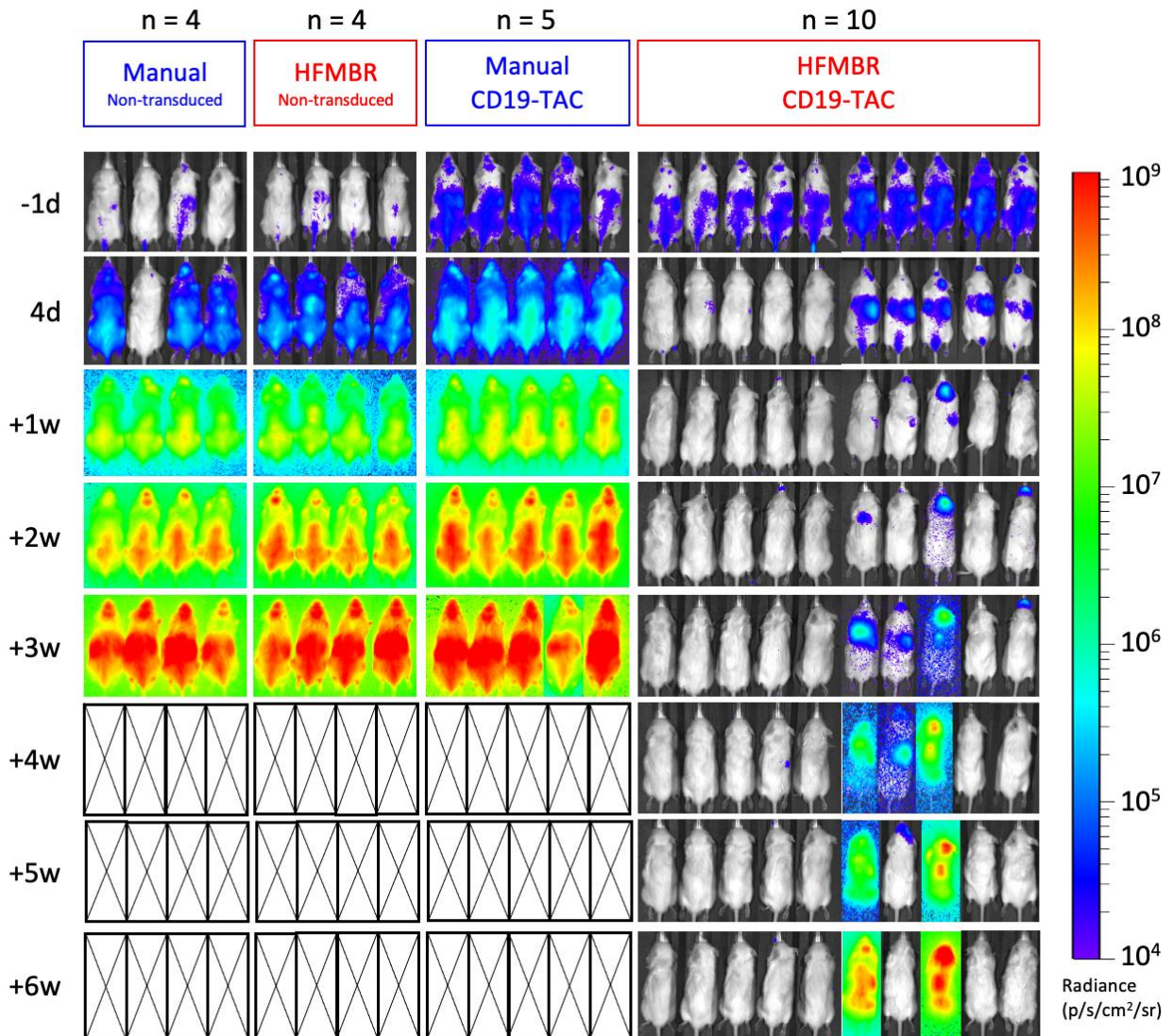
**Supplemental Figure 5. Transduction efficiency in manual and HFMBR production.** PBMC from five donors were manufactured using either the manual method or the HFMBR method in parallel. Each production run involved a single donor's PBMC, was performed independently, and HFMBR and manual processes were performed in parallel. The T cells in production runs #1 - #4 were engineered with a chimeric antigen receptor (CAR) specific for HER-2. The T cells in production runs #5 - #8 were engineered with a T cell antigen coupler (TAC) specific for CD19. At the end of manufacturing, T cells were collected and the frequency of CD8+ (right-hand panel) and CD4+ (left-hand panel) T cells that expressed the CAR or TAC was assessed. A paired students t-test revealed no significant differences between the HFMBR and manual groups.



**Supplemental Figure 6. NALM-6 tumor burden in mice treated with high dose CD19-TAC T cells produced using HFMBR or Manual methods.** NRG mice bearing *firefly* luciferase-expressing NALM-6 tumor cells were treated with  $4 \times 10^6$  CD19-TAC T cells produced using the HFMBR or Manual method. Control mice received an equal number of manufacturing method-matched non-transduced T cells. Tumor burden was monitored over time by bioluminescent imaging on an IVIS Spectrum, following administration of luciferin. Imaging timepoints in days (d) or weeks (w) post-treatment are shown; mice were imaged 1d prior to treatment (pre-ACT), 3 or 4d post-treatment, and weekly thereafter. Data was pooled from 3 independent experiments. Tumor burden from individual mice, as quantified in **Figure 3A**, are shown. An “X” indicates the mouse did not survive until the imaging time point.

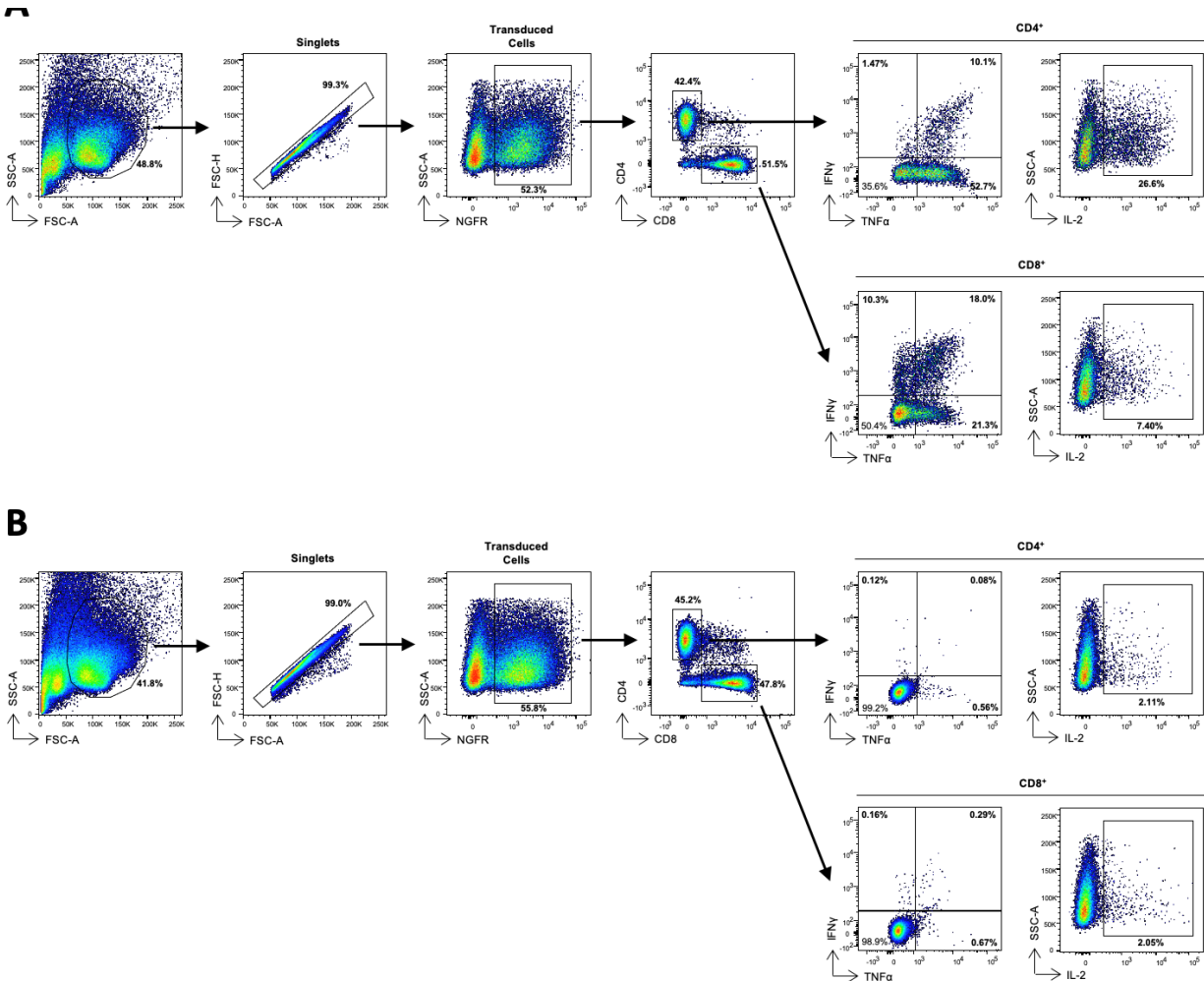


**Supplemental Figure 7. Therapeutic efficacy of CD19-TAC T cells produced using HFMBR or Manual methods.** NRG mice bearing NALM-6 cells were treated with 1.5 x 10<sup>6</sup> CD19-TAC T cells produced using the HFMBR or manual methods. Control mice received an equal number of non-transduced T cells produced under the same conditions. All T cell products were produced from the same donor in parallel. Tumor burden was measured as luminescence produced by the tumors following intraperitoneal administration of luciferin to the tumor-bearing mice. Five mice were treated in each group that received non-transduced T cells and five - nine mice were treated in each group that received CD19-TAC T cells. The fraction of mice without tumor at the end of the experiment are shown in the left-hand corner of each graph.

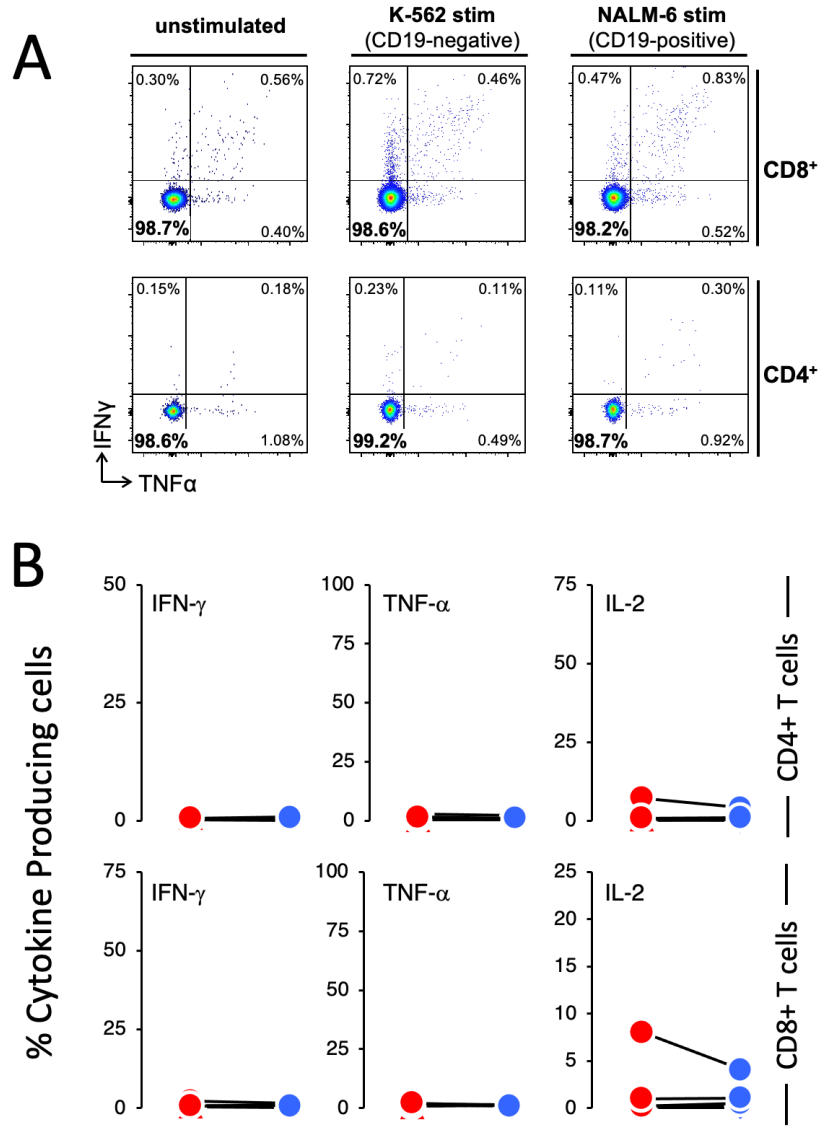


**Supplemental Figure 8. NALM-6 tumor burden in mice treated with low dose CD19-TAC T cells produced using HFMBR or Manual methods.** NRG mice bearing *firefly* luciferase-expressing NALM-6 tumor cells were treated with  $1.0-1.5 \times 10^6$  CD19-TAC T cells produced using the HFMBR or Manual method. Control mice received an equal number of manufacturing method-matched non-transduced T cells. Tumor burden was monitored over time by bioluminescent imaging on an IVIS Spectrum, following administration of luciferin. Mice were imaged prior to treatment, 4d post-treatment, and weekly (w) thereafter. Tumor burden from individual mice, as quantified in **Supplemental Figure 7**, are shown. An “X” indicates the mouse did not survive until the imaging time point.





**Supplemental Figure 9. Representative data and gating strategy for the functional analysis of T cells by intracellular cytokine staining.** T cells engineered with HER2-CAR were manufactured using the manual method. To assess antigen-specific responses, the engineered T cells were co-cultured with tumor cells for 4-hours in the presence of a protein transport inhibitor. The frequency of engineered T cells producing IFN- $\gamma$ , TNF- $\alpha$ , and IL-2 was assessed by intracellular cytokine staining and flow cytometry. **Panel A.** Engineered T cells were co-cultured with SKOV-3 (HER2+) tumor cells. The gating strategy used for analysis of cytokine production is shown. **Panel B.** The same engineered T cells were co-cultured with a HER2- tumor cell line (LOX-IMVI). This data was used to determine gate placement, separating cytokine-negative from cytokine-positive cells.



**Supplemental Figure 10. Non-transduced T cells do not demonstrate antigen-specific cytokine production.** Non-engineered T cells were manufactured using the HFMBR or manual methods. To assess antigen-specific responses, the engineered T cells were co-cultured with tumor cells for 4-hours in the presence of a protein transport inhibitor. The frequency of engineered T cells producing IFN- $\gamma$ , TNF- $\alpha$ , and IL-2 was assessed by intracellular cytokine staining and flow cytometry. **Panel A.** Non-engineered T cells manufactured in an HFMBR were co-cultured in medium alone (unstimulated), with K562 cells (CD19-negative) or with NALM-6 (CD19-positive). Flow cytometry data were gated as shown in **Supplemental Figure 9**. Data for IFN $\gamma$  and TNF $\alpha$  is shown. **Panel B.** Non-engineered T cells were stimulated with either the HER2-positive SKOV-3 cells (circles) or CD19-positive NALM-6 cells (diamonds). T cells manufactured using the manual method are shown in blue and T cells manufactured using the HFMBR method are shown in red. The frequency of T cells producing IFN- $\gamma$  (*left-hand panels*), TNF- $\alpha$  (*central panels*) and IL-2 (*right-hand panels*) are shown. A

total of 5 products generated from 3 different donors were tested. The data were generated from 5 independent experiments. No statistical differences were determined using a paired Students t-test.

GeneSet	Description	TAC	NT
		p-value	p-value
<b>Down-regulated in Bioreactor</b>			
GSE11057_CD4_EFF_MEM_VS_PBMC_UP	Genes up-regulated in comparison of effector memory T cells versus peripheral blood mononuclear cells (PBMC).	4.93E-02	3.51E-02
GSE11057_EFF_MEM_VS_CENT_MEM_CD4_TCELL_UP	Genes up-regulated in comparison of effector memory T cells versus central memory T cells from peripheral blood mononuclear cells (PBMC).	1.23E-02	9.47E-03
GSE11057_NAIVE_VS_EFF_MEMORY_CD4_TCELL_DN	Genes down-regulated in comparison of naive T cells versus effector memory T cells.	4.93E-02	3.80E-02
GSE26928_CENTR_MEMORY_VS_CXCR5_POS_CD4_TCELL_UP	Genes up-regulated in comparison of CD4 central memory T cells versus CD4 CXCR5+ T cells.	3.51E-02	2.21E-02
GSE11924_TH1_VS_TH2_CD4_TCELL_DN	Genes down-regulated in comparison of Th1 cells versus Th2 cells.	9.46E-03	1.4E-02
<b>Up-regulated in Bioreactor</b>			
GSE16522_MEMORY_VS_NAIVE_CD8_TCELL_DN	Genes down-regulated in comparison of rested memory CD8 T cells from pmel-1 mice versus rested naive CD8 T cells from pmel-1 mice.	1.85E-02	1.23E-02
GSE21360_NAIVE_VS_SECONDARY_MEMORY_CD8_TCELL_UP	Genes up-regulated in CD8 T cells: naive versus 2' memory.	6.40E-03	6.40E-03
GSE21360_SECONDARY_VS_QUATERNARY_MEMORY_CD8_TCELL_DN	Genes down-regulated in memory CD8 T cells: 2' versus 4'.	6.74E-03	6.40E-03
GSE22886_NAIVE_CD4_TCELL_VS_MEMORY_TCELL_UP	Genes up-regulated in comparison of naive CD4 T cells versus unstimulated memory CD4 CD8 T cells.	9.82E-03	6.74E-03
GSE23321_CD8_STEM_CELL_MEMORY_VS_CENTRAL_MEMORY_CD8_TCELL_UP	Genes up-regulated in CD8 T cells: stem cell memory versus central memory.	6.74E-03	6.40E-03
KAECH_DAY8_EFF_VS_MEMORY_CD8_TCELL_DN	Genes down-regulated in effector CD8 T cells at the peak expansion phase (day 8	3.51E-02	4.66E-02

	after LCMV-Armstrong infection) compared to memory CD8 T cells (day 40+ after LCMV-Armstrong infection)		
GSE24574_BCL6_HIGH_TFH_VS_TCONV_CD4_TCELL_UP	Genes up-regulated in BCL6 [GeneID=604] high follicular helper T cells versus T conv cells.	4.1E-02	3.5E-02
GSE33425_CD161_INT_VS_NEG_CD8_TCELL_DN	Genes down-regulated in CD8 T cells: KLRB1 int versus KLRB1- .	2.1E-02	3.3E-02
GSE9650_EFFECTOR_VS_EXHAUSTED_CD8_TCELL_DN	Genes down-regulated in comparison of effector CD8 T cells versus exhausted CD8 T cells.	1.4E-02	9.5E-03
GSE9650_GP33_VS_GP276_LCMV_SPECIFIC_EXHAUSTED_CD8_TCELL_UP	Genes up-regulated in comparison of virus specific (gp33) exhausted CD8 T cells versus the virus specific (gp276) cells.	4.1E-02	3.4E-02

**Table I. Immunological gene sets significantly regulated in both TAC and NT in bioreactor.** ssGSEA was performed using MSigDB C7 collection of immunological gene sets. Next, differential regulation of these gene sets was examined by using limma. Only corrected p-values < 0.05 were examined further (see Methods). Gene sets significantly regulated in both TAC and NT are presented in the table. Gene sets related to T cell memory are highlighted in yellow.